Strong stabilization of liquid amorphous calcium carbonate by ovalbumin: gaining insight into the mechanism of 'polymer-induced liquid precursor' processes

SUPPORTING INFORMATION

Stephan E. Wolf, Jork Leiterer, Vitaliy Pipich, Raul Barrea, Franziska Emmerling* and Wolfgang Tremel*

Experimental Section

A suspension of $CaCO_3$ (*p.a.*, Sigma Aldrich) in ultrapure water (Millipore Synergy 185 with UV photo oxidation, 18.2 MΩ/cm) was treated with carbon dioxide (Westfalen AG) over night. The obtained saturated solution of calcium bicarbonate was filtered with a cascade of syringe filters, which consists of a 0.1 µm Millipore Millex VV followed by 20 nm Millipore Anotop in series. Afterwards, the filtrate was treated again with carbon dioxide to dissolve nuclei with diameters < 20 nm. The resulting calcium bicarbonate concentration was about 9.8 $mM \cdot L^{-1}$. Shortly before levitation, the desired protein (ovalbumin Grade V, lysozyme from chicken egg white; Sigma Aldrich) was dissolved in the saturated solution of calcium bicarbonate at the desired concentration. Then, one droplet of the solution with a volume of approximately 4 µL was manually injected in the ultrasonic levitator (Tec5, Oberursel, Germany).

In situ wide-angle X-ray scattering experiments were performed at the µSpot beamline at the synchrotron facility of BESSY II (Helmholtz Centre Berlin for Materials and Energy), featuring monochromatic radiation (λ = 1.00257 Å) with a photon flux of about 10^9 s^{-1} and a beam diameter of

20 μm. Further information concerning the general setup are given by Paris *et al.* (2006) The scattering pattern from corundum served as external calibration standard. No mathematical 'desmearing' of the experimental scattering intensity function was needed due to the small beam diameter of the incident beam. Defining the scattering vector $q = 4\pi/\lambda \sin(\theta)$ in terms of 2θ between incident and scattered radiation of the wavelength λ, the data were processed and converted into diagrams of scattering intensities *I* versus *q* by means of FIT2D (Hammersley *et al.* 1996). Avrami analysis was conducted with OriginPro 8, fitting the background-corrected and normalized integral intensity of the (104) reflex to the Weibull function $I = a - (a - b)\,\mathrm{e}^{-(kt)^d}$, where *t* is the levitation time, and *a*, *b*, *k* and *d* were parameters.

TEM investigations were carried out at a Phillips EM 420 running at 120 kV, equipped with an ORCA-ER Camera (1024 × 1024 pixel) and run with AMT Image Capture Engine v5.42.540a. SEM investigations were performed with a Zeiss DSM 940 running at 10 kV.

An immunogold labeling protocol was applied which based on the micro-scale protocol of Harris (1991): In all steps of washing, a saturated calcium bicarbonate solution was used in order to reduce re-dissolution of the LACC droplets, which was the main issue in these labeling experiments. After the desired time of levitation, the respective droplet was transferred on a lacey-coated TEM grid (Plano, Germany), washing it once and fixate by incubating the sample at 48° C for 48 h. Then, the sample was blocked with 10% purified casein protein (western blocking reagent, Roche, Germany) and then directly incubated with a 1:1000 dilution of the primary antibody (IgG fraction of anti-ovalbumin, antibodies-online GmbH) for 5 min, omitting a washing step to reduce again re-dissolution of the LACC droplets. After rinsing the sample three times, the sample was incubated with a 1:50 dilution of the secondary Anti-Rabbit IgG gold-labeled antibody (Sigma, Germany) for 5 min. Before the final drying of the sample, it was rinsed three times but this time the washing buffer was gradually diluted with ultrapure water (1:0, 1:1, 0:1). This consecutive dilution of the washing buffer was important in order to anticipate crystallization of calcium carbonate arising in the buffer during drying. As the first negative

test, sample with no protein were immunogold labeled which could not withstand the washing steps. As a second negative test, a sample containing 7.5 $mg \cdot mL^{-1}$ ovalbumin was immunogold labeled but with the skip of the primary antibody. The labeling ratio was obtained by counting the gold nanoparticles in a given surface area (droplet-associated or not) of the TEM micrographs and normalizing to the values to the non-bound fraction of nanoparticles. The TEM analysis showed that the LACC droplets did suffer much lesser from the rinsing steps, as they are reduced in number, and that only very sporadically Au-nanoparticles could be found (roughly 1-2 nanoparticles per $3.6 \cdot 10^5$ nm^2).

The X-ray absorption near edge structure was probed at the undulator beamline 18ID of the Advanced Photon Source at Argonne National Laboratory. For details about the beamline, cf. Fischetti *et al* (2004). All spectra were collected in fluorescence mode at room temperature. Peak position in XANES spectra were estimated via their first derivative. Data reduction was accomplished with Athena 0.8.061.

The neutron experiments were carried out at the SANS diffractometer KWS-1 at the FRM II in Garching (more details at JCNS: http://www.jcns.info/jcns_kws1.). The experiments were performed with neutrons of wave length of 6.8 Å with 10% half width of maximum and at sample-to-detector distances 1.3 and 4 m. The scattering data obtained were corrected for background scattering, detection sensitivity of the individual detector channels, and finally evaluated in absolute scale from calibration with a Plexiglas secondary standard.

Employing ScanProsite (De Castro *et al.* 2006) from the ExPASy Proteomics Server, the primary sequence of ovalbumin (PDB-ID: 1OVA) was compared with different Ca-binding motives of EF-hand (ProSite name/number: EF_HAND_1 / PS00018 and EF_HAND_2 / PS50222), C2 (C2 / PDOC00380), S-100 (S100_CABP / PS00303) and annexins (Annexin / PS00223) and no similarity was found.

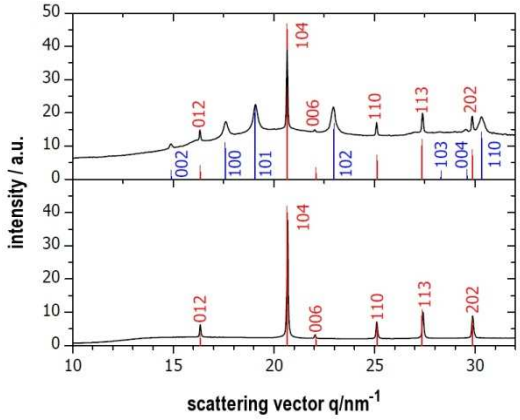

Figure S1 WAXS pattern of the final stages of crystallization (solid line) with corresponding Bragg reflexes of calcium carbonate in the presence of ovalbumin (top) and in absence of protein (bottom). Miller indices are given for calcite (in red) and for vaterite (in blue).

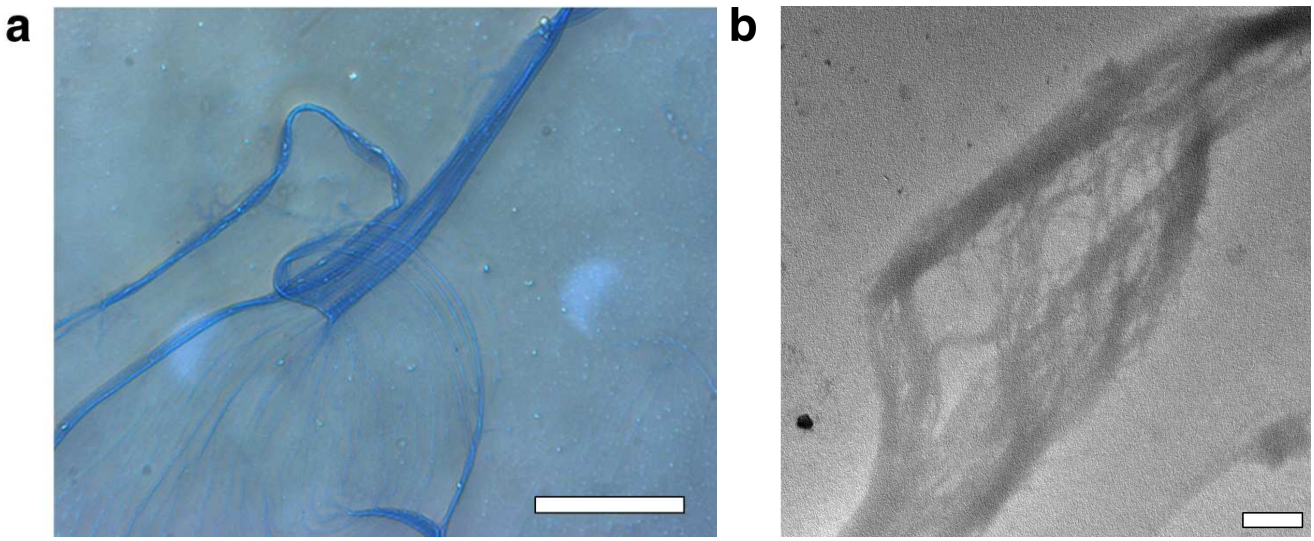

Figure S2 **a)** Standard light (after staining with bromothymol blue) and **b)** transmission electron micrographs of ovalbumin fibrils, whose formation was induced by the addition of calcium chloride. Scale: a) 50 µm, b) 500 nm.

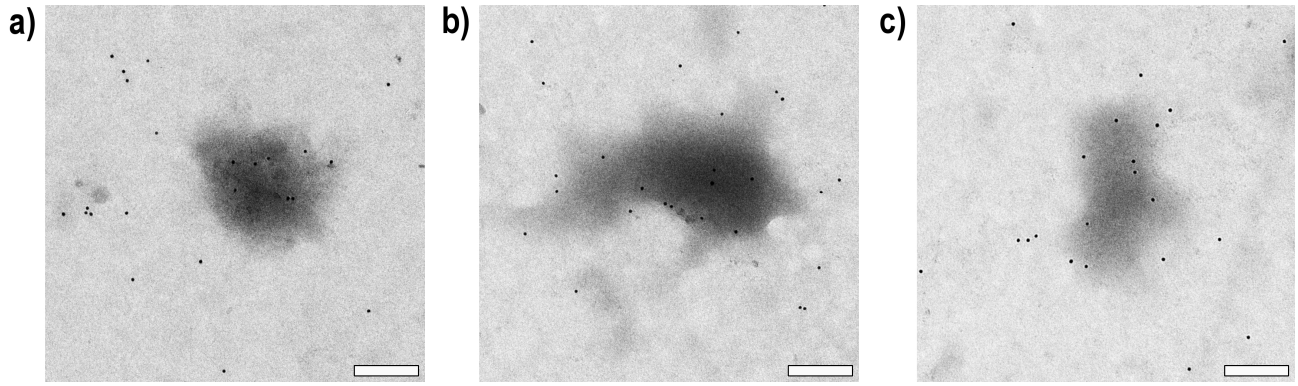

Figure S3 TEM micrographs of samples, which were obtained after 300 s at a protein concentration of 0.5 $mg \cdot mL^{-1}$, indicate after a polyclonal immunogold (IG) labeling that ovalbumin is partially incorporated in the liquid amorphous $CaCO_3$ precursor. Scale: 200 nm.

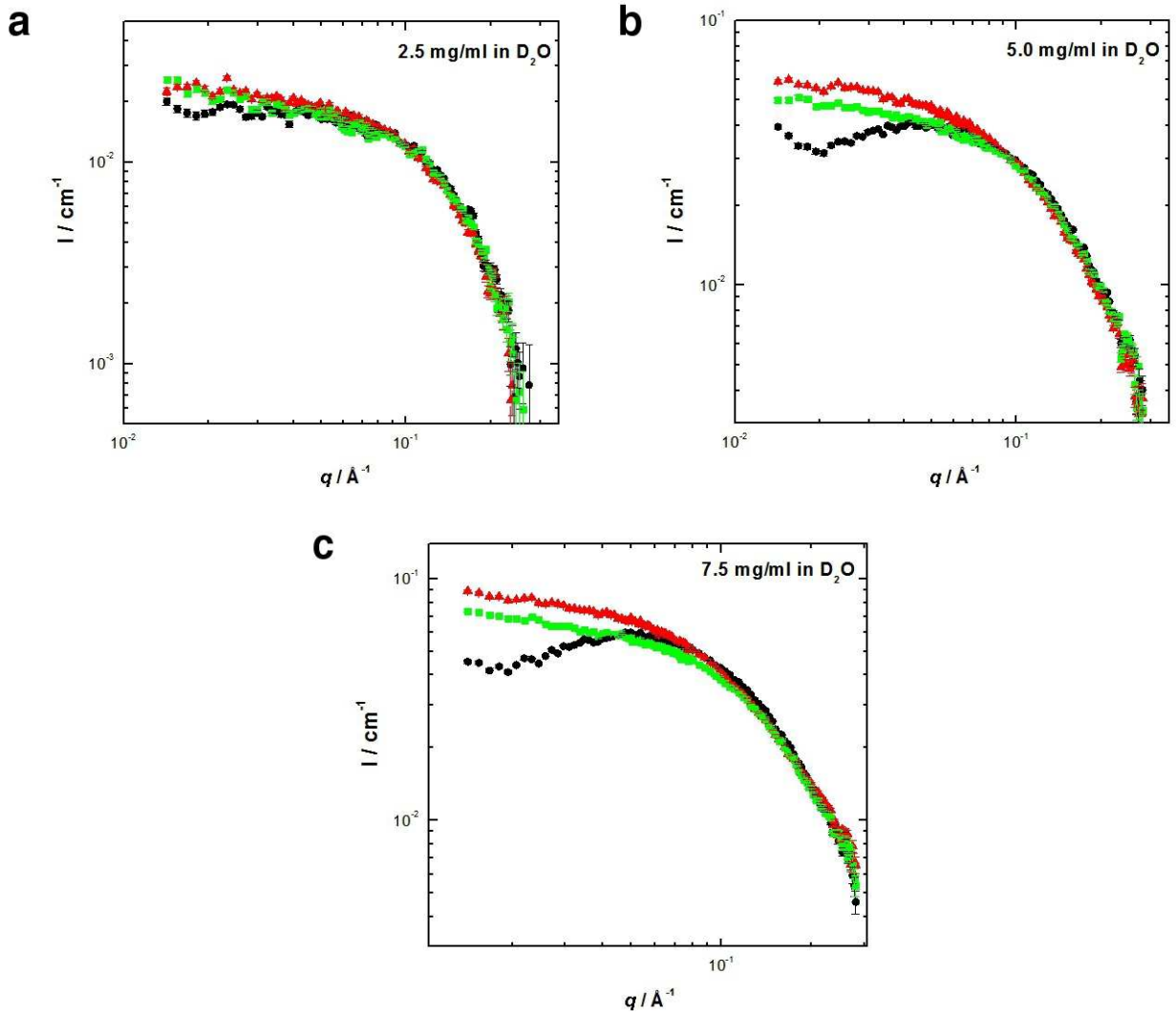

Figure S4 Small-angle neutron scattering of lysozyme at three different concentrations **a)** 2.5 mg·mL^{-1}, **b)** 5 mg·mL^{-1} and **c)** 7.5 mg·mL^{-1}, each in different buffer solutions: ● pure protein, no salt, ▲ 10 mM·L^{-1} $CaCl_2$ and ■ 30 mM·L^{-1} NaCl, i.e. at identical eletric strength as 10 mM·L^{-1} $CaCl_2$. **a)** At 2.5 mg/mL lysozyme all three scatterings curve resemble each other, which means that no loading occurs. **b)** At 5 mg/mL lysozyme slight deviations at $q = 10^{-2}$ Å^{-1} appear. At this point, the structure factor is screened only insufficiently at this salt concentration. However, at higher q, it is clearly visible that at no loading with calcium occurs; there are no differences in the scattering patterns of all three samples. **c)** At the highest concentration of 7.5 mg·mL^{-1} lysozyme, the protein-protein interactions are much more pronounced, they last up to $q = 10^{-1}$ Å^{-1}, but at higher q it is still well perceivable that no loading occurs.

References

Fischetti, R, S Stepanov, G Rosenbaum, R Barrea, E Black, D Gore, R Heurich, et al. (2004): *The BioCAT undulator beamline 18ID: a facility for biological non-crystalline diffraction and X-ray absorption spectroscopy at the Advanced Photon Source.* In: Journal of Synchrotron Radiation 11, 5, 399-405.

Hammersley, A. P., S. O. Svensson, M. Hanfland, A. N. Fitch, and D. Hausermann (1996): *Two-dimensional detector software: From real detector to idealised image or two-theta scan.* In: *High Pressure Research* 14, 4, 235-248.

Harris, R. (1991): *Electron Microscopy in Biology : a Practical Approach*. Oxford, USA: IRL Press, Oxford Univ. Press.

Paris, Oskar, Chenghao Li, Stefan Siegel, Gundolf Weseloh, Franziska Emmerling, Heinrich Riesemeier, Alexei Erko, and Peter Fratzl (2006): *A new experimental station for simultaneous X-ray microbeam scanning for small- and wide-angle scattering and fluorescence at BESSY II.* In: *Journal of Applied Crystallography* 40, 466-470.

De Castro E., Sigrist C.J.A., Gattiker A., Bulliard V., Petra S. Langendijk-Genevaux P.S., Gasteiger E. Bairoch A., Hulo N. (2006): *ScanProsite: detection of PROSITE signature matches and ProRule-associated functional and structural residues in proteins.* In: *Nucleic Acids Res.* 34:W362-W365(2006).